

Separations inside a cube

A.F.F. Teixeira *

Centro Brasileiro de Pesquisas Físicas
22290-180 Rio de Janeiro-RJ, Brazil

November 21, 2018

Abstract

Two points are randomly selected inside a three-dimensional euclidian cube. The value l of their separation lies somewhere between zero and the length of a diagonal of the cube. The probability density $\mathcal{P}(l)$ of the separation is constructed analytically. Also a Monte Carlo computer simulation is performed, showing good agreement with the formulas obtained.

1 Introduction

An important problem in geometry and statistics is: given a convex compact space endowed with a metric, and randomly choosing two points in the space, find the probability density $\mathcal{P}(l)$ that these points have a specified separation l . The study of this problem has a long history [1], and recently gained considerable impetus from researchers in cosmic crystallography [2]-[19].

In a recent paper the functions $\mathcal{P}(l)$ corresponding to $2D$ disks and rectangles were obtained [20]. The methodology introduced in that work is here extended to a $3D$ euclidian cube.

2 Preliminaries

An euclidian cube with side a is assumed, occupying the location $0 < x, y, z < a$ in a cartesian frame. Randomly choosing two points A and B in the cube, we want the probability $\mathcal{P}(l)dl$ that the separation between the points lie between l and $l + dl$. The probability density $\mathcal{P}(l)$ has to satisfy the normalization condition

$$\int_0^{\sqrt{3}a} \mathcal{P}(l)dl = 1. \quad (1)$$

The calculation can be shortened if one considers the symmetries of the cube. Really, if the points A and B have been chosen, imagine the oriented segment $A'B'$ parallel to

*teixeira@cbpf.br

AB , with the tip A' coinciding with the origin O . The other tip B' then lies inside a larger cube, with side $2a$. Since the probability density $\mathcal{P}(l)$ clearly does not depend on which octant of the large cube contains B' , there is no loss in generality in restricting the calculation to the cases where B' is in the octant $0 < x, y, z < a$.

With this assumption, the point B' has cartesian coordinates

$$B' = (l \cos \theta \cos \phi, l \cos \theta \sin \phi, l \sin \theta),$$

where both angles θ, ϕ are bound to the interval $[0, \pi/2]$; here ϕ is the azimuthal angle, while θ is the polar angle measured from the $z = 0$ plane. The corresponding tip B in the original segment must lie inside a parallelepiped with sides (see figure 1)

$$l_x := a - l \cos \theta \cos \phi, \quad l_y := a - l \cos \theta \sin \phi, \quad l_z := a - l \sin \theta. \quad (2)$$

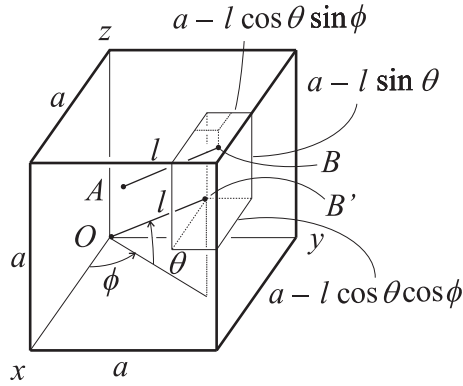


Figure 1 The endpoint B of the segment AB must lie inside the parallelepiped with a corner at $B'(l, \phi, \theta)$.

The probability $\mathcal{P}(l, \theta, \phi) dl d\theta d\phi$ that the segment AB has length between l and $l + dl$, azimuth between ϕ and $\phi + d\phi$, and polar angle between θ and $\theta + d\theta$ is then

$$\mathcal{P}(l, \theta, \phi) dl d\theta d\phi = k l_x l_y l_z l^2 \cos \theta dl d\theta d\phi, \quad (3)$$

where k is a constant and where the assumption $0 < \phi, \theta < \pi/2$ stands. Performing the angular integrations we shall obtain

$$\mathcal{P}(l) = \iint \mathcal{P}(l, \theta, \phi) d\theta d\phi, \quad (4)$$

and we finally fix k using the condition (1).

To calculate $\mathcal{P}(l)$, three cases need be separately considered, depending on the value of l relative to a : namely the cases $0 < l < a$, $a < l < \sqrt{2}a$, and $\sqrt{2}a < l < \sqrt{3}a$.

3 The case $0 < l < a$

As is seen in the figure 2, in this case we effectively have $\phi_{min} = \theta_{min} = 0$, and $\phi_{max} = \theta_{max} = \pi/2$. Then

$$\mathcal{P}(l < a) = k l^2 \int_0^{\pi/2} l_z \cos \theta d\theta \int_0^{\pi/2} l_x l_y d\phi \quad (5)$$

$$= \frac{k l^2}{8} [4\pi a^3 - 6\pi a^2 l + 8al^2 - l^3], \quad (6)$$

where $k = 8/a^6$ as will be fixed later on.

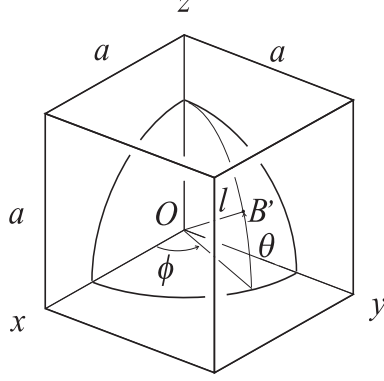


Figure 2 The triangular intersection of the 2D sphere with radius l and centre O with the 3D cube having side $a > l$.

4 The case $a < l < \sqrt{2}a$

In this case the intersection of the 2D sphere (with radius l) with the 3D cube (with side a) is an hexagonal surface as in figure 3.

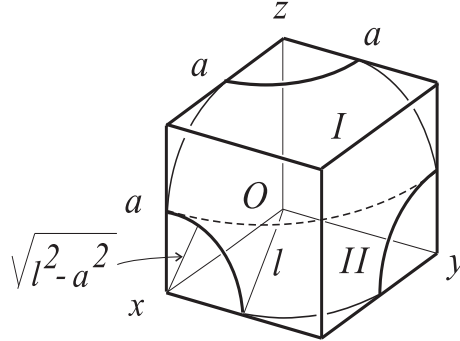


Figure 3 The hexagonal intersection of a 2D sphere with radius l and centre O with a 3D cube with a vertex in O and having side a such that $a < l < \sqrt{2}a$.

We note that the arcs of circle drawn on the faces $x, y, z = 0$ have radius l , while those drawn on the faces $x, y, z = a$ have radius $\sqrt{l^2 - a^2}$.

For convenience of integration we divide the intersection into two regions. In region I we have $\cos^{-1}(a/l) < \theta < \sin^{-1}(a/l)$ and $0 < \phi < \pi/2$.

In region II we have $\theta_{min} = 0$ and $\theta_{max} = \cos^{-1}(a/l)$. To have $\phi_{min}(\theta)$ we note that the circle drawn on the face $x = a$ satisfies the equation $\cos \phi \cos \theta = a/l$, so

$$\phi_{min}(\theta) = \cos^{-1} \left(\frac{a}{l \cos \theta} \right) =: \phi_1(\theta). \quad (7)$$

On the other hand, the circle drawn on the face $y = a$ satisfies $\sin \phi \cos \theta = a/l$, so we have

$$\phi_{max}(\theta) = \sin^{-1} \left(\frac{a}{l \cos \theta} \right) =: \phi_2(\theta). \quad (8)$$

We then find

$$\begin{aligned} & \mathcal{P}(a < l < \sqrt{2}a) \\ &= k l^2 \left[\int_{\cos^{-1}(a/l)}^{\sin^{-1}(a/l)} \cos \theta d\theta \int_0^{\pi/2} d\phi + \int_0^{\cos^{-1}(a/l)} \cos \theta d\theta \int_{\phi_1(\theta)}^{\phi_2(\theta)} d\phi \right] l_x l_y l_z \quad (9) \\ &= \frac{k l}{8} \left[2l^4 + 6a^2 l^2 - a^4 - 2\pi a^3 (4l - 3a) - 8a(2l^2 + a^2) \sqrt{l^2 - a^2} \right. \\ & \qquad \qquad \qquad \left. + 24a^2 l^2 \cos^{-1}(a/l) \right], \quad (10) \end{aligned}$$

where $k = 8/a^6$ as will be fixed later on.

5 The case $\sqrt{2}a < l < \sqrt{3}a$

In this case the 2D sphere with radius l intersects the 3D cube with side a in the triangular surface shown in figure 4.

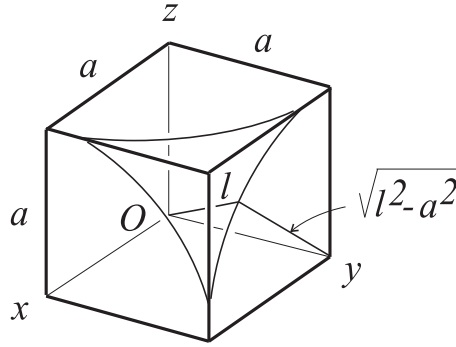


Figure 4 The triangular intersection of a 2D sphere with radius l and centre O with a 3D cube with a vertex in O and having side a such that $\sqrt{2}a < l < \sqrt{3}a$.

As before, the circles drawn on the faces $x, y, z = a$ have radius $\sqrt{l^2 - a^2}$. The azimuthal integration is performed between $\phi_1(\theta)$ and $\phi_2(\theta)$ as in the region II of the preceding case, and again $\sin \theta_{max} = a/l$; but now $\cos \theta_{min} = \sqrt{2}a/l$. We then find

$$\begin{aligned} \mathcal{P}(\sqrt{2}a < l < \sqrt{3}a) &= k l^2 \int_{\cos^{-1}(\sqrt{2}a/l)}^{\sin^{-1}(a/l)} l_z \cos \theta d\theta \int_{\phi_1(\theta)}^{\phi_2(\theta)} l_x l_y d\phi \quad (11) \\ &= \frac{k l}{8} \left[8a(l^2 + a^2) \sqrt{l^2 - 2a^2} - (l^2 + a^2)(l^2 + 5a^2) + 2\pi a^2 (3l^2 - 4al + 3a^2) \right. \\ & \qquad \qquad \qquad \left. + 24a^3 l \sec^{-1}(l^2/a^2 - 1) - 24a^2 (l^2 + a^2) \sec^{-1} \sqrt{l^2/a^2 - 1} \right], \quad (12) \end{aligned}$$

where $k = 8/a^6$.

This value for the constant k derives from the normalization condition (5), namely,

$$\int_0^a \mathcal{P}(l < a) dl + \int_a^{\sqrt{2}a} \mathcal{P}(a < l < \sqrt{2}a) dl + \int_{\sqrt{2}a}^{\sqrt{3}a} \mathcal{P}(\sqrt{2}a < l < \sqrt{3}a) dl = 1. \quad (13)$$

6 Graphs of $\mathcal{P}(l)$

In figure 5 we present a graph of the dimensionless function $a\mathcal{P}(l)$ against the dimensionless variable l/a .

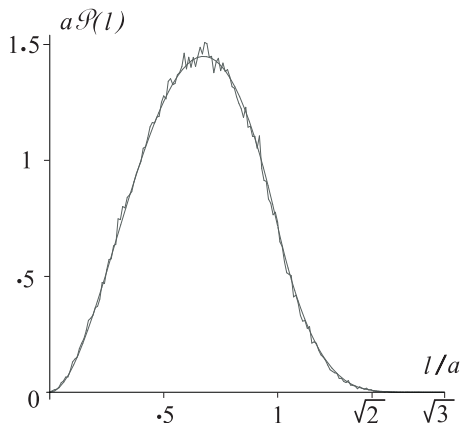


Figure 5 The probability density $\mathcal{P}(l)$ of separation l of pairs of randomly distributed points inside a cube with side a . The irregular curve is the output of a corresponding computer simulation.

We note that the function and its first derivative are continuous in the whole interval $0 < l < \sqrt{3}a$. Nevertheless the second derivative is discontinuous at $l = a$, as discussed in the next section. In the figure a normalized histogram corresponding to 150,000 separations between pairs of points randomly selected in the cube is superimposed, for comparison; the agreement of the two curves evinces the correctness of the calculation.

7 Comments

The integration to find $\mathcal{P}(l)$ in eqs. (5)-(6) is almost trivial; however, not the same can be said about the two other cases, namely in going from (9) to (10) and from (11) to (12). A computer assistance appears paramount in these two cases, to confirm every short step in the calculation and simplification of expressions.

Similarly as in [20], the probability density $\mathcal{P}(l)$ and its first derivative are continuous throughout the entire range $0 < l < \sqrt{3}a$. But the second derivative shows a finite discontinuity at $l = a$, although it is continuous at $l = \sqrt{2}a$.

A remarkable feature of $\mathcal{P}(l)$ is its behaviour for large values of l ; really, near $l = \sqrt{3}a$ we find

$$a\mathcal{P}(l) = \frac{9}{5}(\sqrt{3} - l/a)^5 + O((\sqrt{3} - l/a)^6), \quad (14)$$

so $\mathcal{P}(l)$ is essentially a fifth power of $\sqrt{3} - l/a$. We find that 91% of the separations lie in the range $l \in (0, a)$, 9% lie in the interval $l \in (a, \sqrt{2}a)$, and only 0.04% have $l > \sqrt{2}a$.

References

- [1] Krzysztof Beres, *Distance distribution*, Zeszyty Naukowe Uniwersytetu Jagiellońskiego - Acta Cosmologica - Z. 5 (1976) 7-27
- [2] Kelly A. Farrar & Adrian L. Melott, *Gravity in twisted space*, Computers in Physics, Mar/Apr 1990, 185-189
- [3] Roland Lehoucq, M. Lachièze-Rey & Jean-Pierre Luminet, *Cosmic crystallography*, gr-qc/9604050
- [4] Helio V. Fagundes & Evelise Gausmann, *On closed Einstein-de Sitter universes*, astro-ph/9704259
- [5] Roland Lehoucq, Jean-Pierre Luminet & Jean-Philippe Uzan, *Topological lens effects in universes with non-euclidian compact spatial sections*, astro-ph/9811107
- [6] Germán I. Gomero, Antonio F.F. Teixeira, Marcelo J. Rebouças & Armando Bernui, *Spikes in cosmic crystallography*, gr-qc/9811038
- [7] Helio V. Fagundes & Evelise Gausmann, *Cosmic crystallography in compact hyperbolic universes*, astro-ph/9811368
- [8] Jean-Pierre Luminet & Boudewijn F. Roukema, *Topology of the universe: theory and observation*, astro-ph/9901364
- [9] Jean-Philippe Uzan, Roland Lehoucq & Jean-Pierre Luminet, *A new crystallographic method for detecting space topology*, astro-ph/9903155
- [10] Armando Bernui & Antonio F.F. Teixeira, *Cosmic crystallography: three multipurpose functions*, astro-ph/9904180
- [11] Germán I. Gomero, Marcelo J. Rebouças & Antonio F.F. Teixeira, *Spikes in cosmic crystallography II: topological signature of compact flat universes*, gr-qc/9909078
- [12] Germán I. Gomero, Marcelo J. Rebouças & Antonio F.F. Teixeira, *A topological signature in cosmic topology*, gr-qc/9911049
- [13] Armando Bernui & Antonio F.F. Teixeira, *Cosmic crystallography: the euclidian isometries*, gr-qc/0003063
- [14] Antonio F.F. Teixeira, *Cosmic crystallography in a circle*, gr-qc/0005052
- [15] Roland Lehoucq, Jean-Pierre Luminet & Jean-Philippe Uzan, *Limits of crystallographic methods for detecting space topology*, astro-ph/0005515

- [16] Antonio F.F. Teixeira, *Cosmic crystallography: the hyperbolic isometries*, gr-qc/0010107
- [17] Germán I. Gomero, Marcelo J. Rebouças & Antonio F.F. Teixeira, *Signature for the shape of the universe*, gr-qc/0105048
- [18] Evelise Gausmann, Roland Lehoucq, Jean-Pierre Luminet, Jean-Philippe Uzan & Jeffrey Weeks, *Topological lensing in spherical spaces*, gr-qc/0106033
- [19] Janna Levin, *Topology and the cosmic microwave background*, gr-qc/0108043
- [20] Antonio F.F. Teixeira, *Distances in plane membranes*, physics/0111108